Cover Page

Title: Seismic Multi-Axial Behavior of Concrete-Filled Steel Tube Beam-Columns

Authors: Mark D. Denavit (presenter)
Graduate Research Assistant
Department of Civil and Environmental Engineering
B112 Newmark Civil Engineering Laboratory, MC-250
205 North Mathews Avenue
University of Illinois at Urbana-Champaign
Urbana, Illinois 61801-2352
Telephone: (217) 265-0958
E-mail: denavit2@illinois.edu

Jerome F. Hajjar, Ph.D., P.E.
Professor and Narbey Khachaturian Faculty Scholar
Department of Civil and Environmental Engineering
2129b Newmark Civil Engineering Laboratory, MC-250
205 North Mathews Avenue
University of Illinois at Urbana-Champaign
Urbana, Illinois 61801-2352
Telephone: (217) 244-4027; Fax: (217) 265-8040
E-mail: jfhajjar@illinois.edu

Tiziano Perea
Graduate Research Assistant
School of Civil and Environmental Engineering
790 Atlantic Drive
Atlanta, GA 30332-0355
Georgia Institute of Technology
E-mail: tperea@gatech.edu

Professor Roberto T. Leon
School of Civil and Environmental Engineering
Georgia Institute of Technology
790 Atlantic Drive
Atlanta, GA 30332-0355
Telephone: (404) 894-2220; Fax: (404) 894-2278
E-mail: rleon@ce.gatech.edu

SEISMIC MULTI-AXIAL BEHAVIOR OF CONCRETE-FILLED STEEL TUBE BEAM-COLUMNS

M. D. DENAVIT, J. F. HAJJAR, T. PEREA, and R. T. LEON

ABSTRACT

Accurate nonlinear formulations are necessary for the assessment of structures under seismic loading. A three-dimensional distributed plasticity formulation for both circular and rectangular concrete-filled steel tubes suitable for nonlinear static and dynamic analyses of composite seismic force resisting systems has been developed. The formulation utilizes cyclic constitutive models for the concrete core and steel tube which account for the salient features of each material, as well as the interaction between the two, including concrete confinement and local buckling of the steel tube. A series of experiments on full-scale concrete-filled steel tube beam-columns is also underway at the NEES MAST Laboratory at the University of Minnesota. The specimens were subjected to six-DOF cyclic loading histories intended to explore seismic performance, beam-column interaction strength, and detailed assessment of evolution of cyclic damage in composite beam-columns. Comparisons are made between analytical and experimental results.

INTRODUCTION

Composite columns have been shown to have high strength, stiffness, and ductility. However, little data is available to justify the structural system response factors (e.g., R, C_d, and Ω_o) given in the specifications. In addition, there are significant gaps in the test data particularly related to slender, full-scale composite beam-columns. A current NEES project strives to fill these gaps through developing system response factors; assessing beam-column strength; and establishing guidelines for the computation of equivalent composite beam-column rigidity to be used in seismic analysis and design of composite frames. To these ends, an experimental study and advanced computational models have been developed for investigation of composite beam-column and frame behavior.

FINITE ELEMENT FORMULATION

Three-Dimensional Mixed Beam-Column Element

Frame analyses using distributed-plasticity beam-column elements strike a favorable balance of computational efficiency and accuracy. Tort (2007) developed a three-dimensional mixed beam-column element for the analysis of composite frames that include rectangular concrete-

M. D. DENAVIT and J. F. HAJJAR, Department of Civil and Environmental Engineering, University of Illinois at Urbana-Champaign, Urbana, Illinois, United States.
T. PEREA and R. T. LEON, School of Civil and Environmental Engineering, Georgia Institute of Technology, Atlanta, Georgia, United States.

filled steel tubes (CFT), validating against a large number of experimental tests of composite members and frames. The mixed formulation (treating both element displacements and stress resultants as primary state variables) allows for accurate modeling of both geometric and material nonlinearities. Implemented within the OpenSees framework (OpenSees 2009), the element can be used for static and dynamic analyses of members and frames. The element is formulated in the corotational frame and uses the geometric transformations available in OpenSees.

Uniaxial Cyclic Constitutive Relations for Circular CFT Members

The formulation relies on accurate constitutive relations to achieve accurate results. Several uniaxial constitutive relations have been proposed for circular concrete-filled steel tube (CCFT) members (Sakino et al. 2004; Elremaily and Azizinamini 2002; Susantha et al. 2001; Hatzigeorgiou 2008). Each of these models uses different assumptions and methods of calibration, but they generally strive to mimic the response of concentrically loaded short CCFT columns.

The constitutive relation for the concrete core is based on the rule-based model of Chang and Mander (1994). The compressive branch was altered to reflect the state of confinement existing in CCFT members. The tensile branch and the cyclic rules were adopted without changes. A set of 24 well-documented experiments on concentrically load short columns were selected for calibration of the constitutive relations. These tests were selected to have combinations of high and low values of steel yield stress, concrete compressive strength, and *D/t* ratio.

The level of confinement experienced by the concrete has a significant impact on the behavior of CCFT members. The calibration set was thus used to determine an expression for confinement. The confinement pressure is written in terms of the hoop stress in the steel tube, expressed in terms of the yield stress (i.e., $\alpha_\theta F_y$), and the *D/t* ratio (Eq. (1)). The confined concrete strength is computed using the model of Chang and Mander (1994) (Eq. (2)) for symmetric states of confinement. Noting that the steel is subjected to a biaxial state of stress, the von Mises failure criterion is used to determine the longitudinal strength of the steel tube (Eq. (3)), expressed in terms of the yield stress (i.e., $\alpha_z F_y$). Using these two expressions for concrete stress (Eq. (2)) and steel stress (Eq. (3)), the respective cross sectional areas, and a value for the ratio of hoop stress to yield stress, α_θ, the strength of the column is computed. To determine an expression for the α_θ, a least squares optimization was performed selecting the coefficients to reduce the error between computed strength and experimental strength for the calibration set. The experimental strength was taken as the peak load attained during the test or, for specimens that display continual hardening behavior, an estimation was made of the load at which the cross section was fully inelastic. The best correspondence between computed and experimental strength was found when using a linear function of the *D/t* ratio (Eq. (4)).

$$f_l = \alpha_\theta F_y \frac{2}{D/t - 2} \tag{1}$$

$$f'_{cc} = f'_c\left(-1.254 + 2.254\sqrt{1 + 7.94\left(f_l / f'_c\right)} - 2.0\left(f_l / f'_c\right)\right) \tag{2}$$

$$\alpha_z F_y = \left(\frac{1}{2}\left(\alpha_\theta + \sqrt{4 - 3\alpha_\theta^2}\right)\right) F_y \tag{3}$$

$$\alpha_\theta = -0.138 + 0.00174\left(D/t\right) \tag{4}$$

The backbone stress-strain curve for the concrete is based on the model of Tsai (Chang and Mander 1994), which is defined by the initial slope E_c, peak coordinate (ε'_{cc}, f'_{cc}), and r factor. The initial slope and strain at peak stress are defined using expressions from the literature (Eq. (5) and (6)) (Chang and Mander 1994). The r factor, which controls the nonlinear descending branch, was calibrated such that the energy represented by the computed force-deformation response was equal to the corresponding energy obtained from the experiments. The expression for r based on concentrically loaded short columns was then adjusted to attain better correspondence for other testing configurations including beams and beam-columns; the final expression is shown in (Eq. (7)).

$$E_c\left[\text{MPa}\right] = 12,400 + 500\, f'_c\left[\text{MPa}\right] \tag{5}$$

$$\varepsilon'_{cc} = \varepsilon_c\left(1 + 5\left(f'_{cc}/f'_c - 1\right)\right) \tag{6}$$

$$r = 0.4 + 0.016\left(D/t\right)\left(f'_c/F_y\right) \tag{7}$$

The steel model is based on the bounding-surface plasticity model of Shen et al. (1995). Several modifications were made to model the behavior of cold formed steel tubes. First, to model the built-in residual stress from cold-forming, an initial plastic strain of 0.0006 is assumed, this value was obtained through comparisons with tensile coupon tests of cold-formed steel tube. Second, the backstress of the initial yield surface was shifted to account for the presence of hoop stresses described by Eq. (4). Additional modifications were made to model local buckling. Local buckling is assumed to initiate when a certain critical strain (Eq. (8)), based on results of concentrically loaded short columns where the initiation of local buckling is explicitly indicated, has been reached. For strains higher than the local buckling strain, the response is assumed to be a linear descending branch followed by a constant residual stress branch. The constant residual stress (Eq. (9)) is based on the stress at the occurrence of local buckling and a slenderness parameter, R (Eq. (10)); the form of this equation is based on Bradford et al. (2002). The slope of the linear descending branch is taken as E_s/30. The residual stress and descending slope were both calibrated to obtain correspondence to the calibration set of concentrically loaded short columns.

$$\varepsilon_{lb} = \left(F_y/E_s\right)\left(0.214R^{-1.41}\right) \tag{8}$$

$$F_{res} = \begin{cases} R_{crit}F_{lb}/R & \text{for } R > R_{crit} = 0.17 \\ F_{lb} & \text{otherwise} \end{cases} \tag{9}$$

$$R = \left(D/t\right)\left(F_y/E_s\right) \tag{10}$$

To validate the model, a large number of comparative analyses were performed. Sets of experimental data grouped by loading type were assembled. The loading types include: concentrically loaded short column (additional to the calibration set), bending, proportionally loaded beam-columns, non-proportionally loaded beam-columns, and cyclic. Figure 1 shows three representative samples of the validation studies. The proportionally loaded specimen

subjected a beam-column to eccentric axial load with an identical eccentricity at each end; the non-proportionally loaded specimen subjected the beam-column to constant axial force followed by equal moments at each end to cause single-curvature flexure. The cyclic specimen subjected the beam to cyclic equal moments at each end.

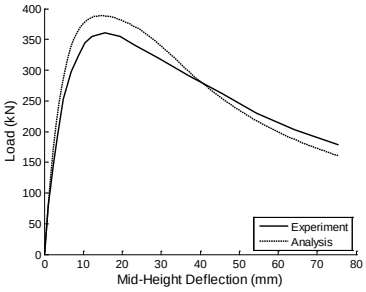

Proportionally Loaded Beam-Column; Kilpatrick and Rangan 1999; Specimen SC-9; F_y = 410 MPa; f'_c = 58 MPa; D/t = 42.4; L/D = 19.1; $ecc./D$ = 0.098

(a)

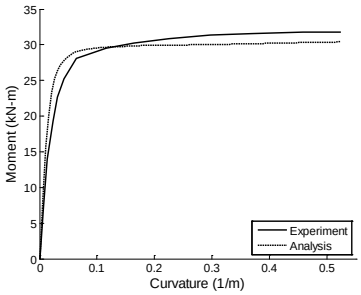

Non-Proportionally Loaded Beam-Column; Fujimoto et al. 2004; Specimen EC4-A-4-035; F_y = 283 MPa; f'_c = 39.9 MPa; D/t = 50.7; L/D = 3.0; P/P_o = 0.35

(b)

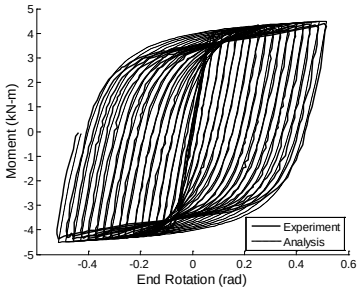

Cyclically Loaded Beam; Elchalakani and Zhao 2008; Specimen F19I1; F_y = 413 MPa; f'_c = 23.1 MPa; D/t = 20.5; L/D = 13.3

(c)

Figure 1. Representative Model Validation Results

FULL-SCALE CFT BEAM-COLUMN TESTS

A series of full-scale concrete-filled steel tube (CFT) beam-column tests is currently underway at the NEES MAST Laboratory at the University of Minnesota. The specimens were selected to fill gaps in prior experimental research, namely to have high member slenderness and high section slenderness (D/t ratio). Parameters in the experimental study include: section shape and size, member length, concrete strength. Table 1 shows a test matrix with nominal geometric and material properties.

The experimental program has a variety of objectives, including: 1) documenting the progression of flexural rigidity ($EI_{effective}$) of the composite section at different load levels; 2) experimentally determining the beam-column interaction strength, including stability effects; 3) investigating post-peak behavior and evolution of damage of members subjected to large cyclic deformations; and 4) providing a complex, well-documented set of data for validation of computational models.

The MAST Laboratory allows for six degrees-of-freedom (DOF) control through a rigid steel crosshead. For the main portion of testing, most specimens were kept in a fixed-free (K=2) configuration, achieved as follows. The beam-column bases are welded to a base plate which is bolted to the testing floor, providing a fixed connection. The beam-column tops are welded to a base plate with a hole for placing the concrete, which is bolted to the crosshead. The free condition is provided by control of the crosshead; allowing horizontal displacements and disallowing bending moments at the top. Twist is constrained to zero due to the low torsional stiffness.

The load protocol is divided into several load cases. The first three load cases are the same for each of the specimens. The first load case subjects the specimen to concentric load. The horizontal DOFs are held at zero force, allowing the specimen to displace transversely. The

vertical DOF is loaded under displacement control until a critical load is reached or until actuator load limits are reached. The second and third load cases subject the specimen to constant axial load (with different values being used between the second and third load cases) and cyclic transverse displacements, causing uniaxial flexure. The vertical DOF is under load control while the horizontal DOFs are under displacement control. To meet the varied objectives of the experimental program, several options were made for the fourth and later load cases. In each of these cases, the general control scheme is that same as that of the second and third load cases. One option involves sets of "probes" of the interaction surface. While holding a constant axial load, the horizontal displacements are increased with a fixed ratio of X to Y displacement until a critical flexural strength is reached, at which point the horizontal displacements are reversed. The process is then repeated for several additional X/Y displacement combinations. Another option subjects the specimen to constant axial load and a prescribed cyclic biaxial horizontal displacement pattern. Table 1 identifies the pattern adopted for these later loading cases.

Table 1. Experimental Test Matrix

Testing Order	$D_{nominal}$ (mm)	$B_{nominal}$ (mm)	$t_{nominal}$ (mm)	$D/t_{nominal}$	$F_{y,nominal}$ (MPa)	$f'_{c,nominal}$ (MPa)	Length (mm)	Later Load Cases
1	141	n/a	3.40	41.5	290	34.5	5486	n/a
2	324	n/a	6.35	51.0	290	34.5	5486	probes
3	508	n/a	6.35	80.0	290	34.5	5486	probes
4	508	305	7.94	64.0	317	34.5	5486	probes
5	508	305	7.94	64.0	317	34.5	5486	probes
6	324	n/a	6.35	51.0	290	82.7	5486	probes
7	508	n/a	6.35	80.0	290	82.7	5486	biaxial cyclic
8	508	305	7.94	64.0	317	82.7	5486	biaxial cyclic
9	508	305	7.94	64.0	317	82.7	5486	probes
10	141	n/a	3.40	41.5	290	34.5	7925	n/a
11	324	n/a	6.35	51.0	290	34.5	7925	biaxial cyclic
12	508	n/a	6.35	80.0	290	34.5	7925	biaxial cyclic
13	508	305	7.94	64.0	317	34.5	7925	biaxial cyclic
14	508	305	7.94	64.0	317	34.5	7925	biaxial cyclic
15	324	n/a	6.35	51.0	290	82.7	7925	biaxial cyclic
16	508	n/a	6.35	80.0	290	82.7	7925	biaxial cyclic
17	508	305	7.94	64.0	317	82.7	7925	biaxial cyclic
18	508	305	7.94	64.0	317	82.7	7925	biaxial cyclic

COMPARISON OF EXPERIMENTAL AND ANALYTICAL RESULTS

The results of Specimen 3 will be discussed in this section as representative of the results to date. Load cases 1 through 3 were as described above with axial loads of 4,448 kN and 2,224 kN in the second and third load cases respectively. Load cases four through six were each a set of eight probes at axial loads of 5,560 kN, 3,336 kN, and 1,112 kN. Two full cycles were performed in each of load cases 2 and 3, the moment at the base is plotted against the top deformation in the direction of motion (Figure 2a & Figure 2b). In these plots, at each pause or reversal, a very stiff response is seen; this is the result of friction in the loading crosshead. Under this particular

loading protocol a number of critical loads were also attained. Assuming that minimal damage had occurred to the specimen, each of these points may be assumed to lie on the experimental interaction surface and may be plotted in three-dimensional stress-resultant space (P-$M_{x,base}$-$M_{y,base}$) (Figure 2c).

Using the finite element formulation, comparable results were attained. A model was created using measured material and geometric properties (Figure 2d). Four elements with three integration points each were used along the height of the column. The loading history of the first three load cases was applied. Analytical results from load cases 2 and 3 are shown superimposed on experimental results in Figure 2a and Figure 2b respectively. For clarity, only data from obtained at the prescribed load level is shown, hiding transitions between load cases. The results show good correspondence between experimental and analytical in stiffness and peak moment. As expected, the stiff response due to crosshead friction at reversals is not seen in the analytical data. Using the same model, an analytical interaction surface has been created (Figure 2c). The interaction surface is the locus of critical loads attained from separate proportionally loaded beam-column analyses. Again, good correspondence is seen between the experimental and analytical results. This indicates that the assumption that minimal damage occurs during the load protocol is valid for this specimen. These results also further validate the accuracy of the element formulation.

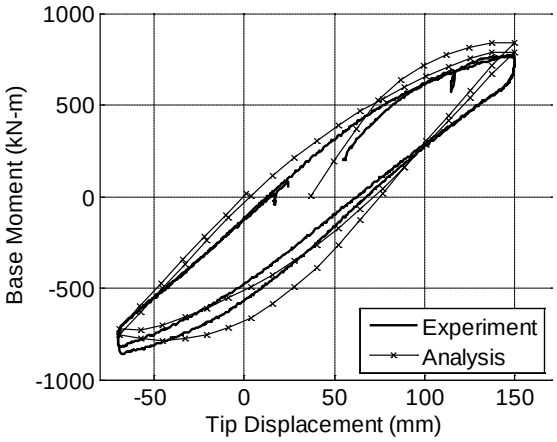

(a) Load Deformation of Load Case 2

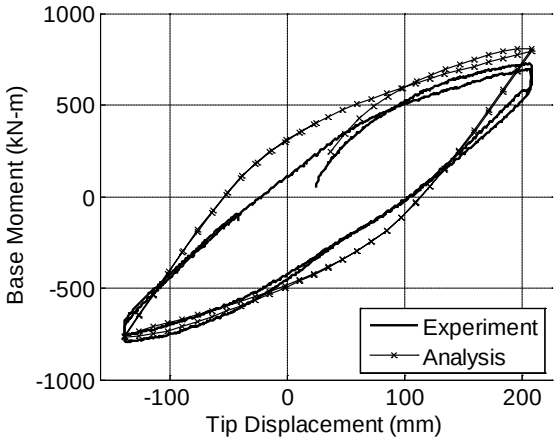

(b) Load Deformation of Load Case 3

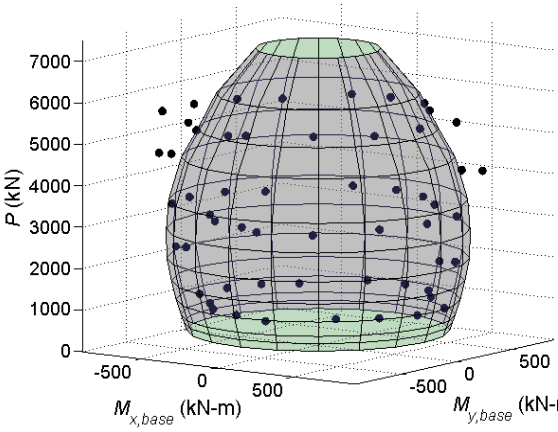

(c) Experimental and Analytical Interaction Surface

Property	Value
D	508 mm
t	6.0 mm
F_y	47.6 MPa
f'_c	5.5 MPa
L	5524 mm
out-of-plumbness	23 mm

(d) Measured Properties

Figure 2. Experimental and Analytical Results of Specimen 3

CONCLUSIONS

Uniaxial constitutive relations for use in distributed-plasticity analyses of circular CFT columns have been presented. These relations, along with the three-dimensional mixed beam-column element comprise an accurate analysis tool for use with composite frames. A series of experiments on full-scale CFT beam-columns is underway. The tests explore several aspects of the behavior of composite columns, including the multi-dimensional interaction surface, biaxial cyclic seismic behavior, and evolution of damage.

ACKNOWLEDGMENTS

The work described here is part of a NEESR project supported by the National Science Foundation under Grant No. CMMI-0619047, the American Institute of Steel Construction, the Georgia Institute of Technology, and the University of Illinois at Urbana-Champaign. In-kind funding was provided by Atlas Tube. Any opinions, findings, and conclusions expressed in this material are those of the authors and do not necessarily reflect the views of the National Science Foundation or other sponsors.

REFERENCES

Bradford, M. A., H. Y. Loh, and B. Uy, 2002, "Slenderness Lmits for Filled Circular Steel Tubes," *Journal of Constructional Steel Research*, 58(2): 243-252.

Chang, G. A. and J. B Mander, 1994, "Seismic Energy Based Fatigue Damage Analysis of Bridge Columns: Part I - Evaluation of Seismic Capacity," National Center for Earthquake Engineering Research, State University of New York at Buffalo. Department of Civil Engineering, Buffalo, New York.

Elchalakani, M. and X.-L. Zhao, 2008, "Concrete-filled Cold-Formed Circular Steel Tubes Subjected to Variable Amplitude Cyclic Pure Bending," *Engineering Structures* 30(2): 287-299.

Elremaily, A. and A. Azizinamini, 2002, "Behavior and Strength of Circular Concrete-filled Tube Columns," *Journal of Constructional Steel Research*, 58(12): 1567-1591.

Fujimoto, T., A. Mukai, I. Nishiyama, and K. Sakino, 2004, "Behavior of Eccentrically Loaded Concrete-Filled Steel Tubular Columns," *Journal of Structural Engineering*, 130(2): 203-211.

Hatzigeorgiou, G. D., 2008, "Numerical Model for the Behavior and Capacity of Circular CFT Columns, Part I: Theory," *Engineering Structures*, 30(6): 1573-1578.

Kilpatrick, A. E. and B. V. Rangan, 1999, "Tests on High-Strength Concrete-Filled Steel Tubular Columns," *ACI Structural Journal* 96(2): 268-274.

OpenSees, 2009, "Open System for Earthquake Engineering Simulation," Open source software, http://opensees.berkeley.edu.

Sakino, K., H. Nakahara, S. Morino, and I. Nishiyama, 2004, "Behavior of Centrally Loaded Concrete-Filled Steel-Tube Short Columns," *Journal of Structural Engineering*, 130(2): 180-188.

Shen, C., I. H. P. Mamaghani, E. Mizuno, and T. Usami, 1995, "Cyclic Behavior of Structural Steels. II: Theory," *Journal of Engineering Mechanics*, 121(11): 1165-1172.

Susantha, K. A. S., H. Ge, and T. Usami, “Uniaxial Stress–strain Relationship of Concrete Confined by Various Shaped Steel Tubes,” *Engineering Structures*, 23(10): 1331-1347.

Tort, C. and Hajjar, J. F. (2007). “Reliability-Based Performance-Based Design of Rectangular Concrete-Filled Steel Tube (RCFT) Members and Frames,” Structural Engineering Report No. ST-07-1, Department of Civil Engineering, University of Minnesota, Minneapolis, Minnesota, August.